Chemical Engineering Journal 162 (2010) 84–90

Contents lists available at ScienceDirect

Chemical Engineering Journal

journal homepage: www.elsevier.com/locate/cej

Synthesis of Fe/MgO nano-crystal catalysts by sol–gel method for hydrogen sulfide removal

Nirattisai Rakmak[a], Wisitsree Wiyaratn[b], Charun Bunyakan[a], Juntima Chungsiriporn[a,*]

[a] Department of Chemical Engineering, Faculty of Engineering, Prince of Songkla University, Haiyai, Songkhla 90112, Thailand
[b] Department of Production Technology Education, Faculty of Industrial Education and Technology, King Mongkut's University of Technology, Tonburi 10140, Thailand

ARTICLE INFO

Article history:
Received 9 November 2009
Received in revised form 1 May 2010
Accepted 4 May 2010

Keywords:
Sol–gel
Hydrogen sulfide
Nano-crystal
Packed column
Fe/MgO

ABSTRACT

The Fe/MgO nano-crystal catalysts were synthesized for removal of hydrogen sulfide (H_2S) in a biogas. The nano-crystalline catalyst supporting powders, magnesium oxide (MgO), were obtained by sol–gel method. Ferric ion from ferric nitrate solution was supported on the MgO nano-crystal powders to give 17.5 nm Fe/MgO crystal size by wet impregnation and calcinations. Catalytic activity for H_2S oxidation was carried out in a semi-batch reactor. Fe/MgO nano-crystal catalysts were held in an aqueous suspension with simulated H_2S gas bubbling for catalytic oxidation and regeneration. The catalysts showed marked catalytic properties such that elemental sulfur was produced during the regeneration with air. Fresh and spent catalysts were characterized by XRD, EDX, FTIR, TEM, and CHNS techniques. The performance of the synthesized Fe/MgO catalysts on H_2S oxidation from a biogas was examined using a packed column scrubber. The results show that the H_2S was specifically absorbed and oxidized by the Fe/MgO catalysts suspension at room temperature. The scrubbing process performed with no absorbing or reaction of CH_4 and CO_2 from the biogas.

1. Introduction

Biogas is a combustible gas produced by anaerobic digestion or fermentation of biodegradable materials such as biomass, manure or sewage at low temperatures. Raw biogas contains about 55–80% methane (CH_4) and 20–45% carbon dioxide (CO_2) with small amounts of water vapor, trace amount of hydrogen sulfide (0–1% H_2S), and other impurities [1]. In industries, a trace amount of H_2S in a gas stream is extremely corrosive to most equipment. Furthermore, incomplete H_2S combustion in biogas burning leads to sulfur dioxide emission which is harmful to the environment, e.g. in the form of acid rain. Commercially, many processes are available for H_2S removal from a gas stream, such as alkaline/amine scrubbing, chemical oxidation, adsorption, bio-filtration, and catalytic wet oxidation [2–4]. The processes that use gas–liquid contactors in which the H_2S is absorbed into complex reagents give either other dissolved sulfide containing components or elemental sulfur as precipitates in the scrubbing solution. These processes have difficulties in the regeneration of the used reagents and are not stable. The H_2S wet oxidation process has been performed using redox mechanisms on Fe-chelating catalysts [5]. However, it has been reported that the Fe-chelating catalytic system requires pH control agents and some stabilizers to stabilize the catalysts. Fe-based catalysts in a heterogeneous catalytic system have potential in the removal and decomposition of H_2S because it can be regenerated by contacting with oxygen. The mechanism of H_2S oxidation on Fe^{3+} catalysts and the regeneration can be shown in Eqs. (1)–(3). The overall reaction of the formation of elemental sulfur from H_2S can be written as Eq. (4) [6]:

$$H_2S \leftrightarrow S^{2-} + 2H^+ \quad (1)$$

$$2Fe^{3+} + S^{2-} \rightarrow S + 2Fe^{2+} \quad (2)$$

$$4Fe^{2+} + O_2 + 4H^+ \rightarrow 4Fe^{3+} + 2H_2O \quad (3)$$

$$2H_2S + O_2 \rightarrow 2S + 2H_2O \quad (4)$$

Fe supported on MgO surface (Fe/MgO) catalysts have been developed in literatures for H_2S removal systems to oxidize H_2S to sulfur at room temperature [2,7,8]. Since MgO has a strongly basic property, it can associate with the base-catalysis in many organic reactions [9]. In addition, a pH control system of the reaction media is not needed [8]. Nanoparticle technology is of considerable interest for a large number of practical applications because it can make metal stronger, harder, and provides high surface area [10,11]. Therefore, nano-crystal MgO powders for supporting Fe^{3+} give further enhancement and useful properties for catalyst applications. In previous work, several routes of nano-crystal MgO synthesis have been used such as sol–gel, hydrothermal, flame spray pyrolysis, laser vaporization, chemical gas phase deposition and surfactant

* Corresponding author.
E-mail address: juntima.c@psu.ac.th (J. Chungsiriporn).

1385-8947/$ – see front matter © 2010 Elsevier B.V. All rights reserved.
doi:10.1016/j.cej.2010.05.001

methods [12]. However, the morphology and properties of the resulting MgO differ and depend largely on the synthesis route and processing conditions. In a practical point of view, the sol–gel method is simple and cost effective.

The aims of this research were to synthesize the Fe/MgO nano-crystal catalysts, characterize the prepared catalysts, and study the performance of the catalyst in H_2S degradation.

2. Materials and methods

2.1. Reagents and chemicals

Analytical grade magnesium nitrate hexahydrate ($Mg(NO_3)_2{\cdot}6H_2O$, 99.5%), oxalic acid ($(COOH)_2{\cdot}2H_2O$, 99.5%) and ferric nitrate ($Fe(NO_3)_3{\cdot}9H_2O$, 98.0%) were obtained from Ajax Finechem. Co., USA. Analytical grade ethanol 99.9% with was obtained from Merk Ltd., Germany. A mixture of 40% of hydrogen sulfide (H_2S) and 60% nitrogen (N_2) in gas cylinder was obtained from Thai Industrial Gases Public Co., Ltd. The biogas stream was obtained from fixed-dome digesters of a pig farm.

2.2. Synthesis of the Fe/MgO nano-crystal catalysts

Fe/MgO catalysts were obtained from two major steps including a synthesis of MgO nano-crystals supporting media and impregnation of Fe^{3+} catalysts on the MgO nano-crystal surface. The MgO nano-crystal material was synthesized according to the sol–gel method described by Kumar and Kumar [13]. First, 200 ml solutions of $Mg(NO_3)_2{\cdot}6H_2O$ and $(COOH)_2{\cdot}2H_2O$ were separately prepared in ethanol and used as precursor materials for MgO nano-crystal synthesis. The $Mg(NO_3)_2{\cdot}6H_2O$ solution was mixed dropwise into the $(COOH)_2{\cdot}2H_2O$ solution with vigorous magnetic stirring and kept vigorously stirred for 12 h. The solution was subsequently dried at 100 °C for 24 h. The reaction scheme of the precursor mixture can be expressed by Eq. (5). The dried reaction mixture was ground and sieved through a 270-mesh screen to get the MgO nano-crystal powders. The calcination was performed for 2 h in air flowing under atmospheric pressure and cooled at a rate of 10 °C/min. The reaction of the calcination step is given in Eq. (6) [13]:

$$Mg(NO_3)_2{\cdot}6H_2O + (COOH)_2{\cdot}2H_2O \rightarrow MgC_2O_4{\cdot}2H_2O + 2HNO_3 + 6H_2O \quad (5)$$

$$MgC_2O_4{\cdot}2H_2O + 0.5O_2 \rightarrow MgO + 2CO_2 + 2H_2O \quad (6)$$

Fe/MgO nano-crystal catalysts were then prepared by wet impregnation of an aqueous solution of $Fe(NO_3)_3{\cdot}9H_2O$ onto the MgO nano-crystal support. Amounts of the raw catalysts were calculated to get 15 wt% Fe^{3+} loading in Fe/MgO nano-crystals. The catalyst mixture was dried at 100 °C for 24 h, ground and sieved through a 270-mesh screen, and calcined at 600 °C for 2 h to obtain the Fe/MgO nano-crystal catalysts.

2.3. Characterizations of the catalysts

To ensure that the nano-crystals of MgO and Fe/MgO catalysts were obtained, Energy Dispersive X-ray Spectrometer (EDS: Oxford ISIS 300) was used. The surface morphology was evaluated using a transmission electron microscope (TEM). X-ray diffraction (XRD) patterns were obtained with the CuKα radiation (λ = 1.5418 Å) which identified the phase(s) and gave the average crystal size of the catalysts. BET surface area of the catalysts was measured by the Surface Area and Pore Size Analyzers (COULTERTM SA3100^{TM}).

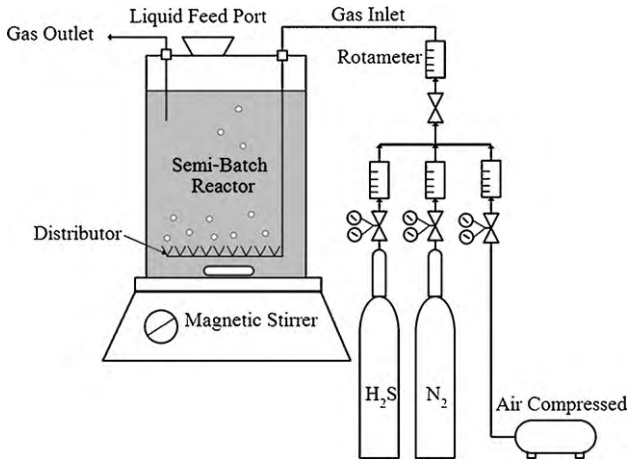

Fig. 1. Schematic diagram of a semi-batch reactor for catalytic activity tests in H_2S removal and degradation.

2.4. Catalytic activity for H_2S oxidation

The Fe/MgO and MgO nano-crystal catalysts activity tests for H_2S removal from a gas phase were carried out in a semi-batch gas scrubbing reactor (Fig. 1) for 60 h at room temperature. A 2 l cylindrical glass reactor (7.5 cm diameter, 20 cm height) with a stirrer (300 rpm) was constructed. Catalytic absorbing solutions were prepared by dispersing the 3 g of the catalysts powder in 1500 ml deionized water and charging to the reactor. The simulated gas, H_2S/N_2 and H_2S/air streams at 1500 ppm H_2S concentration and 2 l/min was continuously bubbled in the liquid absorbent through a gas distributor. The concentrations and flow rates of the simulated gas were controlled using a regulator and a rotameter. To measure the H_2S concentration, samples of the inlet and outlet (or treated) gases were taken during the experiments by absorbing in the impingers (glass bubblers) containing cadmium sulfate ($CdSO_4$) which turned to cadmium sulfide (CdS) when it was contacted with H_2S. The concentrations of H_2S absorbing in the $CdSO_4$ solution were then analyzed by an iodometric method [14]. The H_2S removal efficiency (%) can be determined by Eq. (7) using the concentrations of H_2S in the inlet and outlet streams as follows:

$$\%\,H_2S\ \text{removal} = \frac{H_2S\ \text{inlet} - H_2S\ \text{outlet}}{H_2S\ \text{inlet}} \times 100 \quad (7)$$

where % H_2S removal is the percentage H_2S removal efficiency, H_2S inlet is the inlet H_2S concentration in biogas or absorbent solution and H_2S outlet is the H_2S concentration in biogas or absorbent solution after treated.

The surface properties of the fresh and spent Fe/MgO nano-crystal catalysts characterized by Energy Dispersive X-ray Spectrometer (EDS:Oxford ISIS 300) and Fourier Transform Infrared Spectrometer (FTIR: Model Equinox 55, Burker) obtained by KBr disk method over the wave number range 300–4000 cm^{-1}. The spent catalyst sample was taken after the operation time of 60 h and was prepared for the characterization by filtering through filter papers, rinsing by deionized water, and drying at 100 °C for 24 h. The quantity of sulfur element production from gas absorption in the Fe/MgO nano-crystal catalysts absorbent liquid was taken after the operating time of 12 h and analyzed by CHNS–O analyzer (CE Instruments Flash 1112 Series EA).

2.5. Catalytic performance in H_2S removal from biogas

2.5.1. Continuous scrubbing experimental setup

The quality of Fe/MgO nano-crystal catalysts and the effect of the absorption parameters in H_2S removal from a biogas were studied

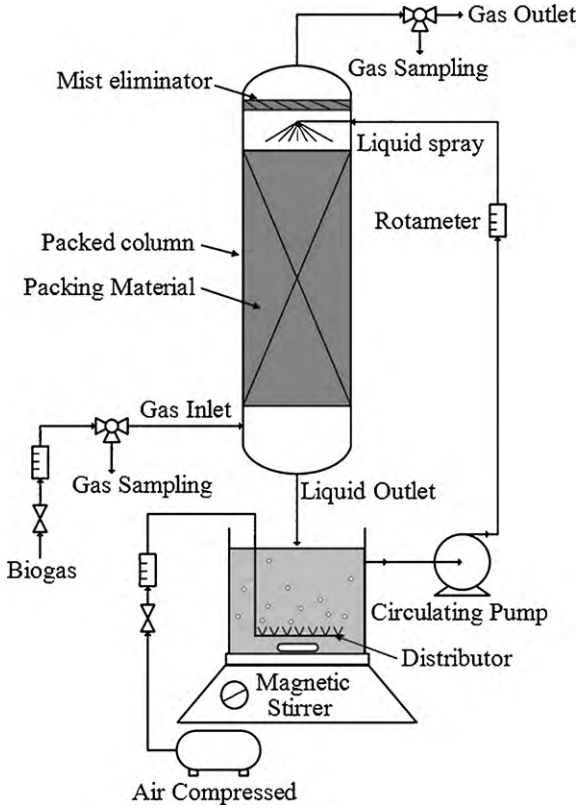

Fig. 2. Schematic diagram of packed column laboratory scale.

using a laboratory scale packed column system. The packed column with the dimension of 5 cm diameter and 65 cm height was constructed using an acrylic cylinder containing rashing ring packing media with the height of 45 cm. The top of the column holds demister packing media with the height of 5 cm to remove entrained liquid droplets from the gas outlet. Schematic diagram of the system that was used for the catalyst verification on H_2S removal from a biogas is shown in Fig. 2.

2.5.2. Experimental parameters

Absorption parameters such as amount of the catalysts, liquid to gas ratio (L/G), air flow rate, and packing media sizes were investigated for the study of the Fe/MgO nano-crystal catalyst performance in H_2S removal and oxidation from biogas. A constant H_2S concentration (1500 ppm) in a biogas stream deriving from a pig farm at 2 l/min was continuously introduced to the packed column for a running time of 60 min. The scrubbing solutions prepared from 1.0 to 3.0 g Fe/MgO nano-crystal catalysts in 500 ml deionized water were re-circulated from the storage tank to the top of the packed column. Counter current flow of the scrubbing liquid to biogas stream was designed at the L/G ratio of 5–20 l/m^3. The spent catalyst solution was collected and regenerated in the storage tank by air bubbling with the flow rates of 5–20 l/min. The effects of packing bead sizes on the absorption performance were also monitored for the packing diameters of 5 and 9 mm.

2.5.3. Analysis of the system performance

Gas samples were taken from 2 points of the inlet and outlet of the column after reaching steady-state conditions of about 10 min from start up and later with a time interval of about 10 min. The amount of H_2S in the gas samples was analyzed by the iodometric method and calculated for H_2S removal efficiency (%) according to Eq. (7). Mass percentages of CH_4 and CO_2 in the biogas before and after treated were determined by gas chromatography using ShinCarbon ST 100/120 micropacked column.

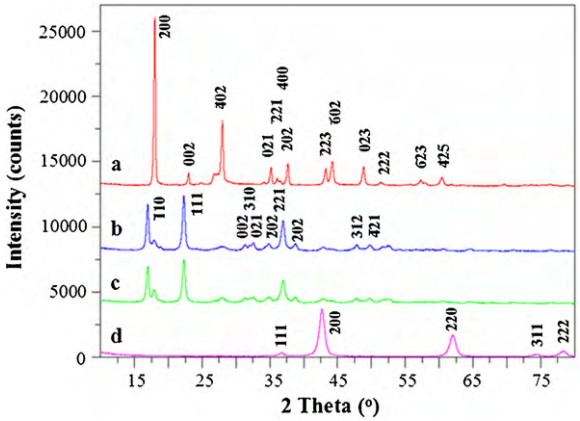

Fig. 3. X-ray diffraction patterns of sol–gel product (1:1 molar ratio of magnesium nitrate and oxalic acid): dried at 100 °C for 24 h (a), after calcinations at 200 °C (b), 400 °C (c) and 600 °C (d) for 2 h.

3. Results and discussion

3.1. MgO catalyst support media

3.1.1. Effects of calcination temperatures on MgO synthesis

The X-ray diffraction pattern of sol–gel precursor powders from the solution of $Mg(NO_3)_2{\cdot}6H_2O$ and $(COOH)_2{\cdot}2H_2O$ after drying at 100 °C for 24 h is shown in Fig. 3a. This diffractogram reveals that the experimental method used in the synthesis yielded a monoclinic structure. The formation of magnesium oxalate dihydrate ($MgC_2O_4{\cdot}2H_2O$) was found with known lattice parameters: a = 12.6750 Å, b = 5.4060 Å, c = 9.9840 Å, α = 90.0000 Å, β = 129.4500 Å, γ = 90.0000 Å and Z = 4.00. The results show that the calcinations of dried precursor powder at 200 and 400 °C for 2 h gave complete removal of crystallizing water and provided magnesium oxalate (MgC_2O_4) as seen in Fig. 3b and c. The formation yielded a monoclinic structure of MgC_2O_4 with the following lattice parameters: a = 9.4130 Å, b = 6.2290 Å, c = 5.7240 Å, α = 90.0000 Å, β = 9.4700 Å, γ = 90.0000 Å and Z = 4.00. The X-ray diffraction pattern of the MgO product obtained from calcination at 600 °C for 2 h is presented in Fig. 3d. This diffraction pattern agrees well with the peaks of standard MgO. This confirms that MgO was formed to high purity from the synthesis. This result also shows that the crystals match with the lattice parameters: a = 4.2198 Å, b = 4.2198 Å, c = 4.2198 Å, α = 90.0000 Å, β = 90.0000 Å, γ = 90.0000 Å and Z = 4.00. A TEM micrograph of the MgO nano-crystals is illustrated in Fig. 4. The result shows that the precursors could be uniformly dispersed and crystallized in the ethanol solvent to form particles with a regular and cubic shape.

3.1.2. Effects of precursor molar ratios on the MgO crystal size

The crystal size of MgO (d, nm) was calculated from the (2 0 0) diffraction peak using the well-known Scherrer equation as shown in Eq. (8):

$$d = \frac{K\lambda}{B\cos\theta} \quad (8)$$

where K is a dimensionless constant that may range from 0.89 to 1.39 depending on the specific geometry of the scattering objects, i.e. for a cubic three-dimensional crystal, K = 0.94 [15]. θ and B variables are the angles between the incident and diffracted beams (°) and the full width at half maximum: FWHM (rad), respectively.

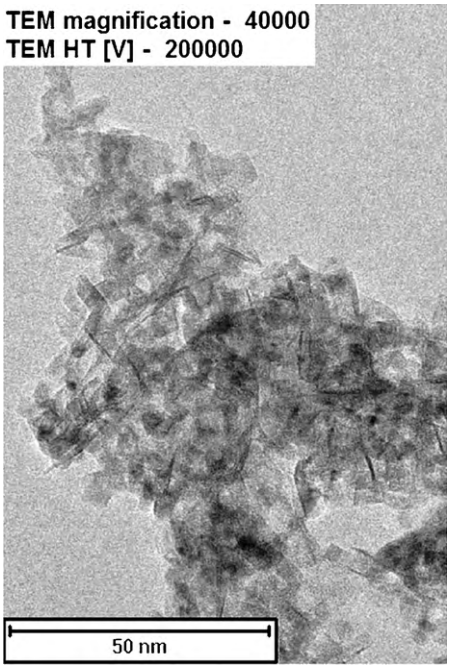

Fig. 4. TEM micrograph of MgO nano-crystals obtained from the calcination at 600 °C for 2 h.

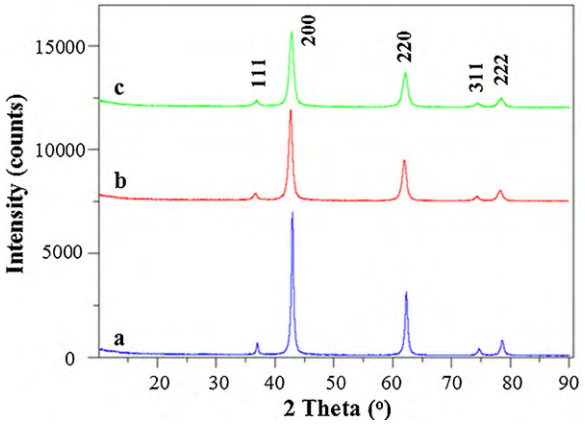

Fig. 5. X-ray diffraction patterns of the sol–gel products with different molar ratios of magnesium nitrate and oxalic acid (a) 1:0.5, (b) 1:0.75, and (c) 1:1 after decomposition at 600 °C for 2 h.

Both variables can be measured from the X-ray broadening. The wavelength of the X-ray is $\lambda = 0.15418$ nm.

Fig. 5 shows the X-ray diffraction pattern of the MgO crystal at different molar ratios of the precursors (magnesium nitrate and oxalic acid) obtained from the calcination at 600 °C for 2 h. Table 1 shows the variables obtained from the diffraction patterns for the MgO crystal size calculation and the calculation results. It was found that the crystal size of MgO was in the range of 12.9–36.3 nm. The precursors follow the reactions (5) and (6) during the drying and calcination process. The smallest MgO crystal size was

Table 1
Calculation variables and MgO crystal sizes at different molar ratios of the precursors.

MgO (ratio)	2θ (°)	B (°)	d (nm)
MgO (1:0.5)	42.85	0.2460	36.3
MgO (1:0.75)	42.78	0.5412	16.5
MgO (1:1)	42.75	0.6888	12.9

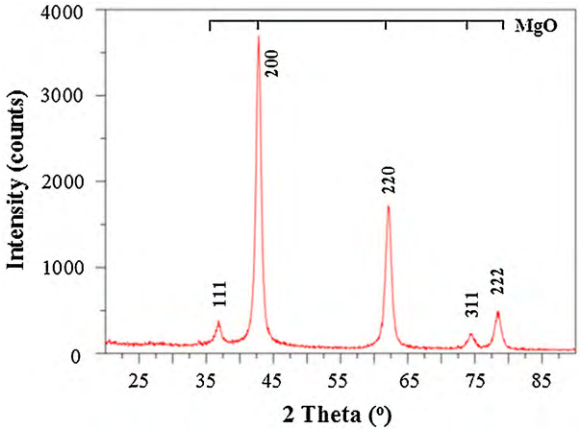

Fig. 6. X-ray diffraction pattern of Fe/MgO after decomposition at600 °Cfor2 h.

obtained with the molar ratio of the precursors of 1:1. In this case, the BET surface area and the pore volume were 178.46 m^2/g and 0.00311 ml/g, respectively.

3.2. Characterization of the Fe/MgO catalysts

Samples of MgO nano-crystal catalysts from the calcining process of 600 °C for 2 h were further used to support Fe^{3+} on the crystal surfaces by a wet impregnation technique. The calculated amount of $Fe(NO_3)_3{\cdot}9H_2O$ was dissolved and loaded to the calcined MgO nano-crystal powders to get 15 wt% loading of Fe^{3+}. The X-ray diffraction pattern of the supported Fe/MgO nano-crystal catalysts is shown in Fig. 6. From the characteristic peaks, only the peaks corresponding to MgO are present. No diffraction peaks of iron compounds such as α-Fe_2O_3 were obtained. The Fe/MgO phase had the same XRD pattern as the pure MgO sample. The EDX spectra from X-ray spectrometer show the elemental Mg, O and Fe on the analysis of Fe/MgO nano-crystal catalysts. The result indicates that Fe^{3+} is present on the MgO surface with ionic bonding. From the XRD data, the Fe/MgO nano-crystal size was calculated to be 17.5 nm. From the BET analysis, the BET surface area and the pore volume were 171.59 m^2/g and 0.00298 ml/g, respectively. The results were not significantly different from those of the pure MgO catalysts. TEM observation of the Fe/MgO nano-crystal catalysts is shown in Fig. 7. It can be seen that the nano-crystal sizes of the catalysts obtained

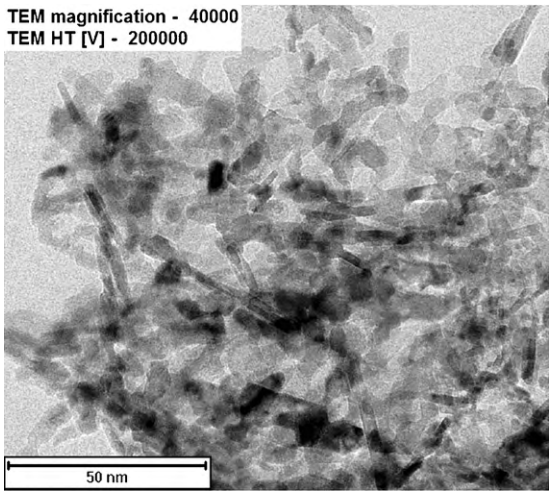

Fig. 7. TEM micrograph of Fe/MsO nano-crystals synthesized via a wet impregnation technique.

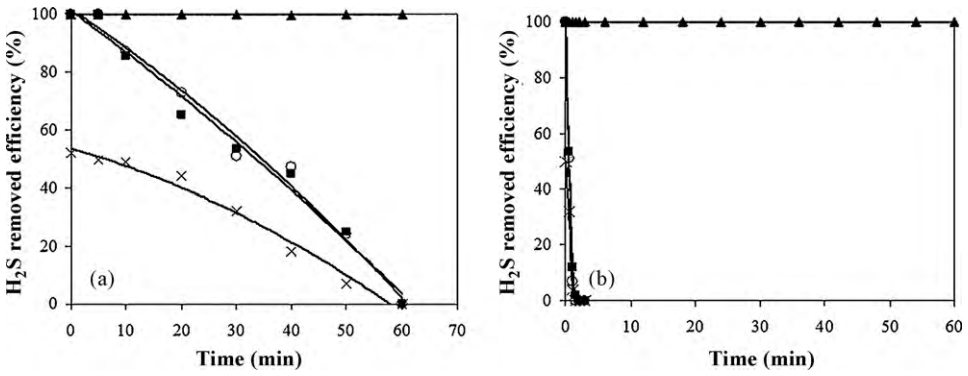

Fig. 8. H:S removal efficiency in a semi-batch reactor using pure deionized water as absorbent (×). MgO absorbent with H_2S air gas stream (○), Fe MgO absorbent with H:S air gas stream (▲), and Fe MgO absorbent with H_2S/N_2 gas stream (■) for the operation times of 1 h (a) and 60 h (b).

by the calcinations at 600 °C as observed on TEM micrographs are consistent with the calculation results.

3.3. Catalytic activity in H_2S oxidation

3.3.1. H_2S oxidation in a semi-batch reactor

A semi-batch reactor was carried out to study the activity of MgO and Fe/MgO nano-crystal catalysts using H_2S simulated gas at room temperature. Fig. 8 shows the H_2S removal efficiency using the three absorbents consisting of pure deionized water, Fe/MgO nano-crystal suspensions, and MgO nano-crystal suspension. Simulated gas streams with H_2S/air and H_2S/N_2 were prepared and introduced to the system. A comparison of the catalytic activity for the use of the air and N_2 simulated gases at 1500 ppm H_2S concentration were performed using the absorbing solution of 3.0 g catalyst/1500 ml. Fig. 8a gives the results of simulated gas feeding of H_2S/air to the MgO absorbent catalysts and H_2S/N_2 to the Fe/MgO absorbent catalysts. The data show that the H_2S removal efficiency reached 100% initially and then decreased to 0% within 1 h. The use of pure deionized water initially yielded 53% removal efficiency and then decreased to 0% within 1 h. However, the feed of the H_2S/air simulated gas to the Fe/MgO absorbent catalysts yielded 100% H_2S removal efficiency throughout the 60 h of the experiments (Fig. 8b). This could not be achieved by the Fe/MgO catalysts prepared by other method [16].

In the case of the H_2S/air simulated gas bubbled in the Fe/MgO absorbent liquid, H_2S reacted with the catalysts and the spent catalysts were regenerated by the O_2 containing in the air. The Fe valence state of ferric ion in the Fe/MgO nano-crystal catalysts is reduced from Fe^{3+} to Fe^{2+} by S^{2-} following the redox cycles and then regenerated back to Fe^{3+} by O_2 via a re-oxidation reaction on the heterogeneous catalysts. These reactions follow the equations given in Eqs. (2) and (3). Therefore, O_2 is necessary for the Fe/MgO nano-crystal catalyst regeneration, and the Fe^{3+} valence on Fe/MgO nano-crystal catalysts is an effective species for the H_2S removal which could not be achieved by MgO alone. For the bubbling of H_2S/N_2 in the Fe/MgO absorbent, the reactions occurred without the catalytic regeneration which resulted in decreasing catalyst activity. For the use of pure deionized water, the water only absorbed H_2S from the gas phase to the liquid absorbent without any reduction of the elemental sulfur. Therefore, the water was saturated with H_2S at the maximum concentration of 2.5 g/l in a short time and could not absorb more H_2S.

3.3.2. Characterization of the fresh and spent catalysts for H_2S degradation

The fresh and spent Fe/MgO nano-crystal catalysts used for H_2S absorption in the semi-batch system were characterized by EDX and FTIR analyzer. In order to investigate the changes on the catalysts caused by H_2S oxidation and O_2 regeneration, samples of the spent catalysts with and without the O_2 feeding into the absorbent solution were collected and analyzed. The fresh catalyst and the catalyst with regeneration samples had the same brown color, while the spent catalyst without regeneration had some black spots on the surface. The EDX characteristic results showed 3 elements consisting of Fe, O, and Mg on the fresh and spent catalysts with regeneration. In contrast, 4 elements consisting of S, Fe, O, and Mg were found in the spent catalysts without regeneration. The appearance of the S element can be determined from the FTIR results provided in Fig. 9. The bands at about 3400 and 1635 cm^{-1} are due to water adsorbed in the pores of the material. The absorption band at 334 cm^{-1} is assigned to Fe–S [17], which indicated that iron sulfide was formed and dispersed on the catalysts. Therefore, the Fe^{3+} valence states in the used Fe/MgO nano-crystal catalysts without regeneration had already degraded by transforming into the iron sulfide form and were not reactive with the H_2S.

The Fe/MgO nano-crystal liquid absorbent absorbed H_2S during the bubbling of H_2S/air simulated gas in the semi-batch reactor and oxidized S^{2-} to elemental sulfur. The CHNS–O analyzer found 38 wt% sulfur in the total solid catalyst sample, which gives the removal capacity of H_2S by the catalyst of 0.68 g sulfur/g catalyst after 12 h reaction time. This result agrees well with the material balance. The pH of the absorption solution was constant at pH 8.8 throughout the experiment (60 h), which did not the affect to Fe(II) oxidation rate in this system at the excess air flow rate for catalyst regeneration.

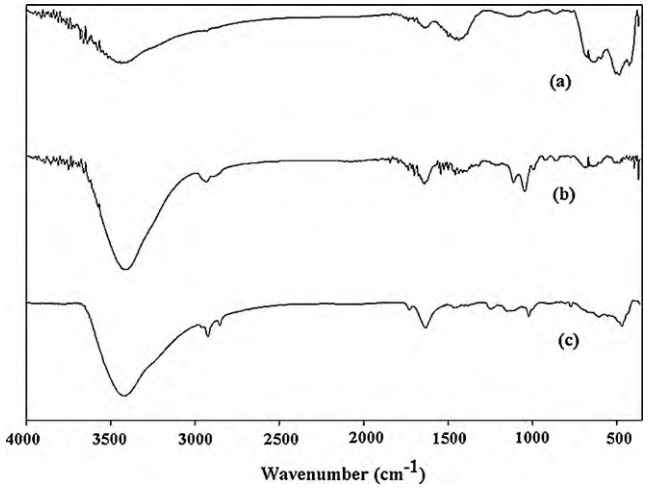

Fig. 9. FITR spectral pattern of fresh catalysts (a), spent catalysts with regeneration (b), and spent catalysts with out regeneration (c).

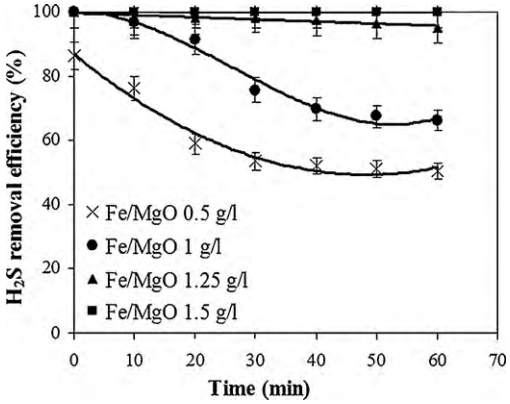

Fig. 10. Effect of Fe/MgO concentrations (g/l) in liquid absorbent of packed column system on the H_2S removal efficiency from biogas.

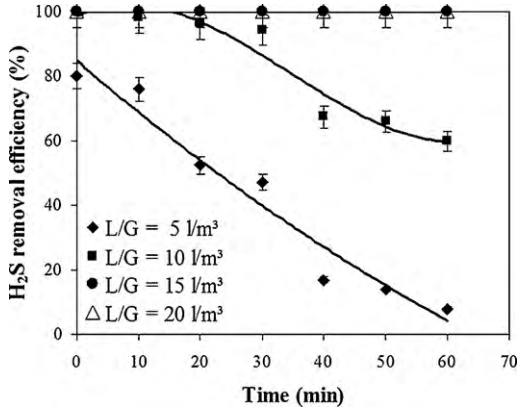

Fig. 11. Effect of L/G ratios on the H_2S removal efficiency by the Fe/MgO heterogeneous catalyst in packed column system.

3.4. H_2S absorption in packed column

From the above results, it was found that the synthesized Fe/MgO nano-crystal catalysts had a good activity on the decomposition of H_2S under the experimental conditions. Thus, it is necessary to conduct further characterizations on these potentially promising catalysts, which can be used for the catalytic decomposition of H_2S in a biogas from pig farms. In this study, a packed column system with a laboratory scale was chosen to test the catalytic performance of the catalysts because it gives low pressure drop and allows high gas flow rate and easy regeneration of the catalysts. It is commonly used for air treatment. The effects of the absorbing parameters on H_2S removal from biogas and the characterizations of the catalysts are explained as follow.

3.4.1. Effects of catalyst concentration on the removal of H_2S from biogas

Fig. 10 shows the removal efficiency of H_2S from the biogas according to the absorption and catalytic reaction by Fe/MgO nano-crystal catalysts absorbent in the packed column system. The catalyst concentration in the liquid absorbent of 1.5 g/l promoted the H_2S degradation with 100% removal efficiency throughout the 60-min run time. The use of 0.5–1.25 g/l catalyst concentrations decreased the removal efficiency of the system with time. It means that the lower concentrations of Fe/MgO nano-crystal catalysts do not provide enough reactive ferric species to oxidize H_2S from the biogas stream which results in the decrease in the absorption efficiency of the catalyst and the degradation rate of H_2S.

3.4.2. Effect of L/G ratios on the H_2S removal from biogas

The L/G ratio is the most important parameter for the design of an absorption column [18]. In this experimental part, the constant gas flow rate was 2 l/min and the liquid flow rate was changed to get the L/G ratio variation range of 5–20 l/m^3. The H_2S removal efficiency by the Fe/MgO heterogeneous catalysts according to the L/G ratios is shown in Fig. 11. The L/G ratio range of 15–20 l/m^3 was the preferable absorption condition because it yielded 100% H_2S removal efficiency over the operating time. H_2S removal efficiency became decreasing with time when the L/G ratios were lower than 15 l/m^3. This is because the higher levels of L/G ratios increase the amount of the absorbing solution flowing across the surface of the packing media which is directly in contact with the gas phase. The mass transfer of H_2S from the gas phase to the liquid absorbent was improved and the absorption performance was increased.

3.4.3. Effect of packing sizes on the H_2S removal from biogas

For rashing ring packing media size variations in the absorption column of 5 and 9 mm diameter, the H_2S removal studies from the biogas stream were carried out at the same conditions of the L/G ratio (20 l/m^3), the H_2S concentration in biogas (1500 ppm), and the dosage of the catalysts in the absorbent (3 g). In principle, the size of the packing material is an important parameter. It has a direct effect on the efficiency of the absorption system because the different packing sizes can change the contacting area and mass transfer between the liquid and gas phase. In these experimental runs for the packing size study, the H_2S removal efficiency was found to be 100% during the tests for both cases. The results show that the range of the controlled packing sizes used in this study did not have a significant effect on the system because they both provided sufficient contacting surface area between the catalyst absorbing solutions and the biogas phase.

3.4.4. The regeneration of the catalysts

In a chemical absorption, H_2S was continuously removed from a biogas stream by catalytic reactions. The ferric ion in the Fe/MgO nano-crystal catalysts is reduced from Fe^{3+} to Fe^{2+} by S^{2-} from H_2S. Regeneration of the spent catalysts containing in the absorbent liquid storage tank was continuously active by the oxygen from the air bubbling. The feed flow rate of the air plays an important role on the Fe/MgO nano-crystal catalyst regeneration as presented in Eq. (3) and Fig. 12. The H_2S removal efficiency was found to be 100% throughout the experiment when the air bubbling was controlled at 15–20 l/min, and the minimum air flux was 15 l/min. There was no obvious evidence of the catalytic activity loss over 1 h making it a promising catalyst for H_2S decomposition. In the case of the air flow rates of 5–14 l/min, the amount of oxygen was not enough for the catalyst regeneration. This results in unsuccessful regener-

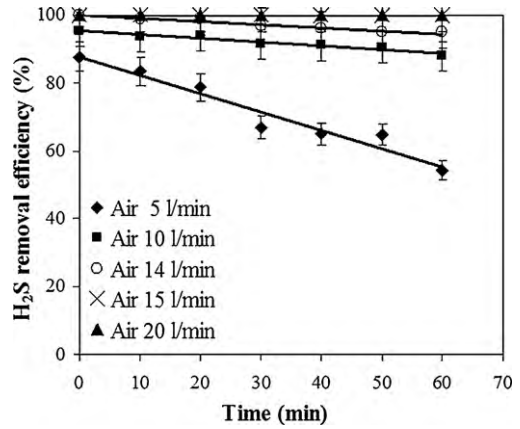

Fig. 12. Effect of bubbling air flow rates on the Fe/MgO nano-crystal catalysts regeneration for the H_2S removal efficiency in a packed column system.

Table 2
Inlet and outlet mass percent composition of biogas from packed column system.

Sample	% CH_4	% CO_2
Inlet	73.87	23.37
Outlet	74.07	20.81

ation of some catalysts. The efficiency for H_2S removal from biogas was found to gradually decrease with the run time especially with the air flow rate of 5 l/min. In this case, the decreasing in the H_2S conversion efficiency was seriously obtained.

3.4.5. Composition of treated biogas

Gas chromatography (CG) was employed to investigate the inlet and outlet biogas compositions of packed column system as shown in Table 2. The result shows that the inlet and outlet concentrations of CH_4 and CO_2 are not significantly different. It indicates that no absorption or reaction of the CH_4 and CO_2 by the Fe/MgO nano-crystal catalysts occurred in the absorbent solution. Thus, Fe/MgO nano-crystal catalysts can effectively be used for the removal of H_2S from a biogas without affecting the main composition of the biogas.

4. Conclusions

The Fe/MgO nano-crystal catalysts were synthesized by a sol–gel method and applied to remove H_2S in a biogas from a pig farm. The successful synthesis yielded MgO nano-crystals with the sizes ranging from 12.9 to 36.3 nm depending on the different molar ratios of the precursors. Fe^{3+} from ferric nitrate solution was supported on the MgO nano-crystals by a wet impregnation technique to give 17.5 nm Fe/MgO crystals. The experimental results in a semi-batch reactor indicated that the Fe/MgO nano-crystal catalysts with regeneration showed marked catalytic properties such that elemental sulfur was produced (0.68 g sulfur/g catalyst). The H_2S removal from a biogas in a packed column scrubber using the Fe/MgO nano-crystal catalysts with a sufficient air flow rate and L/G ratio for the catalyst regeneration shows an outstanding possibility. In addition, the reaction of the catalysts with methane was not observed.

Acknowledgements

The authors would like to thank the Department of Chemical Engineering, Faculty of Engineering and the Graduate school, Prince of Songkla University for equipment and facility, and the Thailand Research Fund for financial support.

References

[1] L.V.-A. Truong, N. Abatzoglou, A H_2S reactive adsorption process for the purification of biogas prior to its use as a bioenergy vector, Biomass Bioenergy 29 (2) (2005) 142–151.
[2] E.-K. Lee, K.-D. Jung, O.-S. Joo, Y.-G. Shul, Influence of iron precursors on catalytic wet oxidation of H_2S to sulfur over Fe/MgO catalysts, J. Mol. Catal. A: Chem. 239 (1–2) (2005) 64–67.
[3] M. Fortuny, J.A. Baeza, X. Gamisans, C. Casas, J. Lafuente, M.A. Deshusses, D. Gabriel, Biological sweetening of energy gases mimics in biotrickling filters, Chemosphere 71 (1) (2008) 10–17.
[4] D. Gabriel, H.H.J. Cox, M.A. Deshusses, Conversion of full-scale wet scrubbers to biotrickling filters for H_2S control at publicly owned treatment works, J. Environ. Eng. -ASCE 130 (10) (2004) 1110–1117.
[5] H.J. Wubs, A.A.C.M. Beenackers, Kinetics of the oxidation of ferrous chelates of EDTA and HEDTA in aqueous solution, Ind. Eng. Chem. Res. 32 (1993) 2580–2594.
[6] D. Graubard, G. Gialet, C. Sexsmith, R. Girard, N. McCagherty, N. Carnegie, ATCO Midstream's Gas Sweetening Experience Using Iron-Redox Technology, Merichem Chemicals & Refinery Services LLC—Gas Technology Products, 2004.
[7] E.-K. Lee, K.-D. Jung, O.-S. Joo, Y.-G. Shul, Selective oxidation of hydrogen sulfide to elemental sulfur with Fe/MgO catalysts in a slurry reactor, B. Kor. Chem. Soc. 26 (2005) 2.
[8] E.-K. Lee, K.-D. Jung, O.-S. Joo, Y.-G. Shul, Support effects in catalytic wet oxidation of H_2S to sulfur on supported iron oxide catalysts, Appl. Catal. A: Gen. 284 (2005) 1–4.
[9] H. Hattori, Catalysis by basic metal oxides, Mater. Chem. Phys. 18 (1988) 533–552.
[10] Y.H. Kim, D.K. Lee, B.G. Jo, J.H. Jeong, Y.S. Kang, Synthesis of oleate capped Cu nanoparticles by thermal decomposition, Colloids Surf. A 284–285 (2006) 364–368.
[11] D. Gulkov, O. Solcov, M. Zdrazil, Preparation of MgO catalytic support in shaped mesoporous high surface area form, Micropor. Mesopor. Mater. 76 (2004) 137–149.
[12] P. Saravanan, R. Gopalan, V. Chandrasekaran, Synthesis and characterisation of nanomaterials, Def. Sci. J. 58 (2008) 504–516.
[13] A. Kumar, J. Kumar, On the synthesis and optical absorption studies of nano-size magnesium oxide powder, J. Phys. Chem. Solids 69 (2008) 2764–2772.
[14] EPA Method 11, Determination of Hydrogen Sulfide Content of Fuel Gas Streams in Petroleum Refineries, CFR 40, Part 60, Appendix A.
[15] B.-Q. Xu, J.-M. Wei, H.-Y. Wang, K.-Q. Sun, Q.-M. Zhu, Nano-MgO: novel preparation and application as support of Ni catalyst for CO_2 reforming of methane, Catal. Today 68 (2001) 217–225.
[16] K.-D. Jung, O.-S. Joo, S.-H. Cho, S.-H. Han, Catalytic wet oxidation of H_2S to sulfur on Fe/MgO catalyst, Appl. Catal. A: Gen. 240 (2003) 235–241.
[17] T. Baird, K.C. Campbell, P.J. Holliman, R. Hoyle, D. Stirling, B.P. Williams, Structural and morphological studies of iron sulfide, J. Chem. Soc., Faraday Trans. 92 (1996) 445–450.
[18] W.L. McCabe, J.C. Smith, P. Harriott, Unit Operations of Chemical Engineering, 7th edition, Mc Graw Hill, 2005, pp. 576–580.